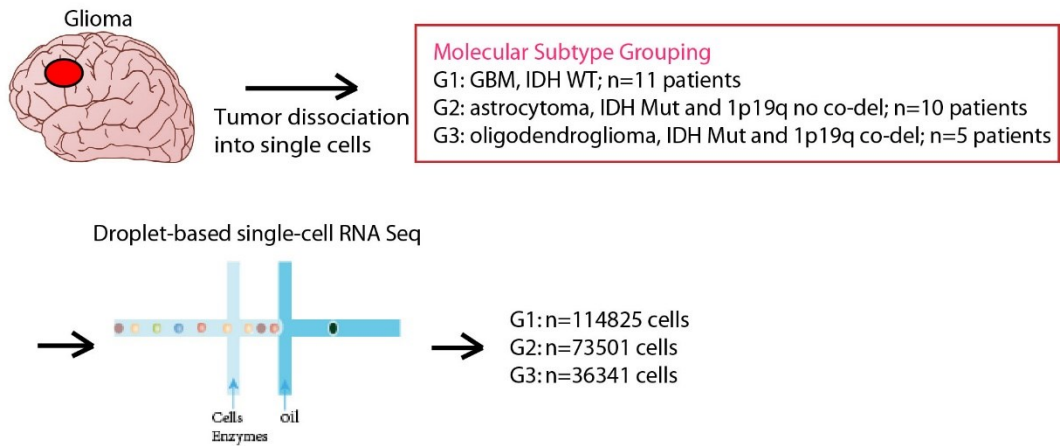


**Distinct immune escape and microenvironment between radial glia-like and primitive oligodendrocyte precursor cell-like glioma revealed by single-cell RNA-seq analysis**

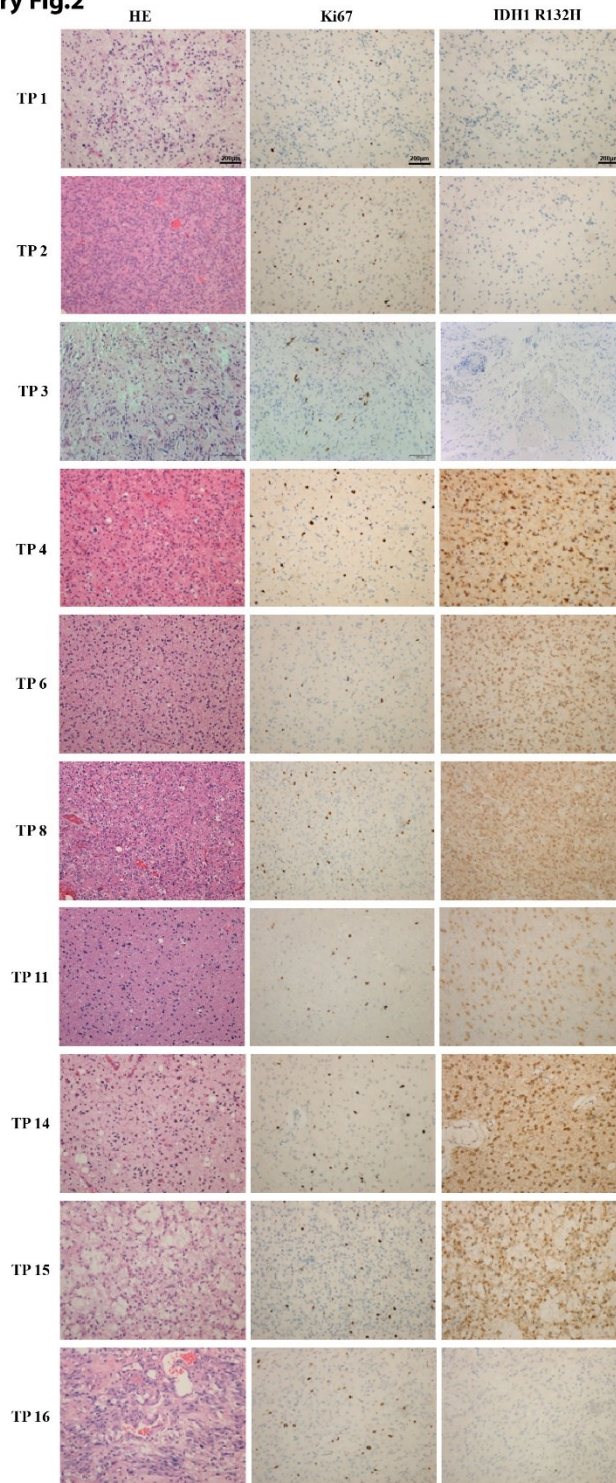
Weiwei Xian<sup>1#</sup>, Mohammad Asad<sup>2#</sup>, Shuai Wu<sup>3#</sup>, Zhixin Bai<sup>1#</sup>, Fengjiao Li<sup>1</sup>, Junfeng Lu<sup>3</sup>, Gaoyu Zu<sup>1</sup>, Erin Brintnell<sup>2</sup>, Hong Chen<sup>4</sup>, Ying Mao<sup>5</sup>, Guomin Zhou<sup>1,6</sup>, Bo Liao<sup>7</sup>, Jinsong Wu<sup>3\*</sup>, Edwin Wang<sup>2\*</sup>, Linya You<sup>1,6\*</sup>

## Supplementary Fig.1



Supplementary Figure 1. **Workflow of single cell RNA seq profiling of 26 glioma from our cohort.** Workflow shows single cell dissociation from freshly resected glioma tissues for generating single-cell RNA-seq profiles and classification of four groups. n=11, 10, 5 were included for G1-G3 to obtain 114825, 73501, 36341 cells before filtering, respectively.

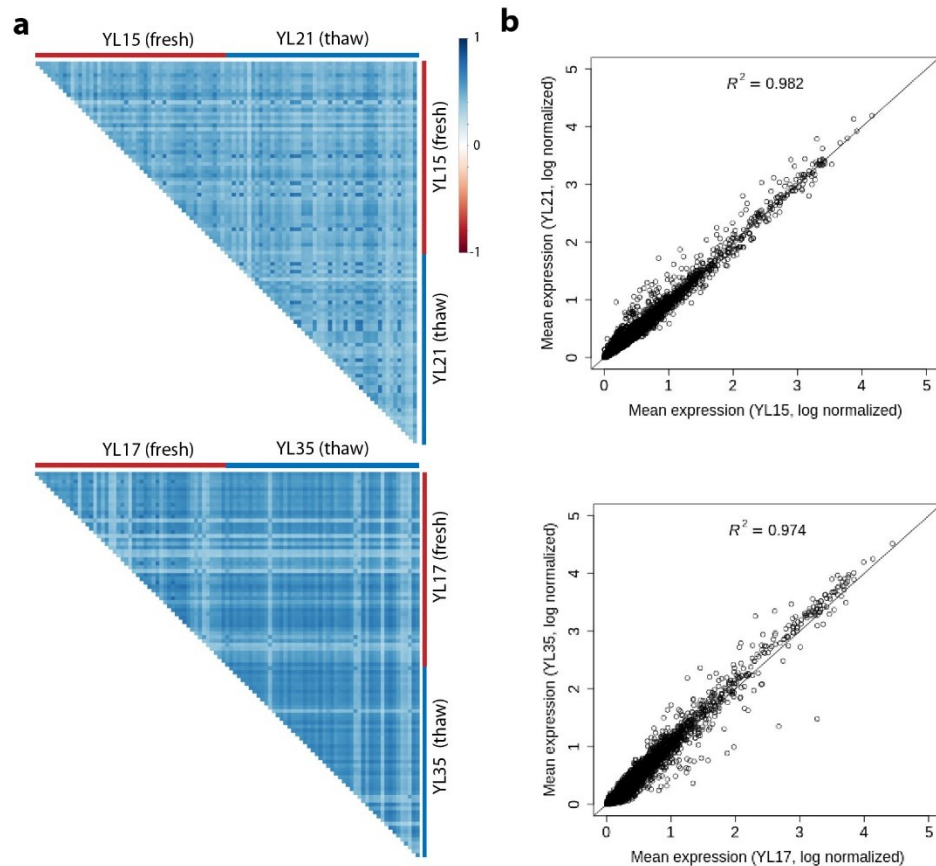
**Supplementary Fig.2**



Supplementary Figure 2. **Representative histology of glioma samples in our cohort.** Left column showed HE staining; middle column indicated Ki67 staining; and right column showed IDH1 R132H staining. All images were with 100x magnification and scale bars indicated 200 $\mu$ m. Note for some samples, IDH1 R132H staining results were

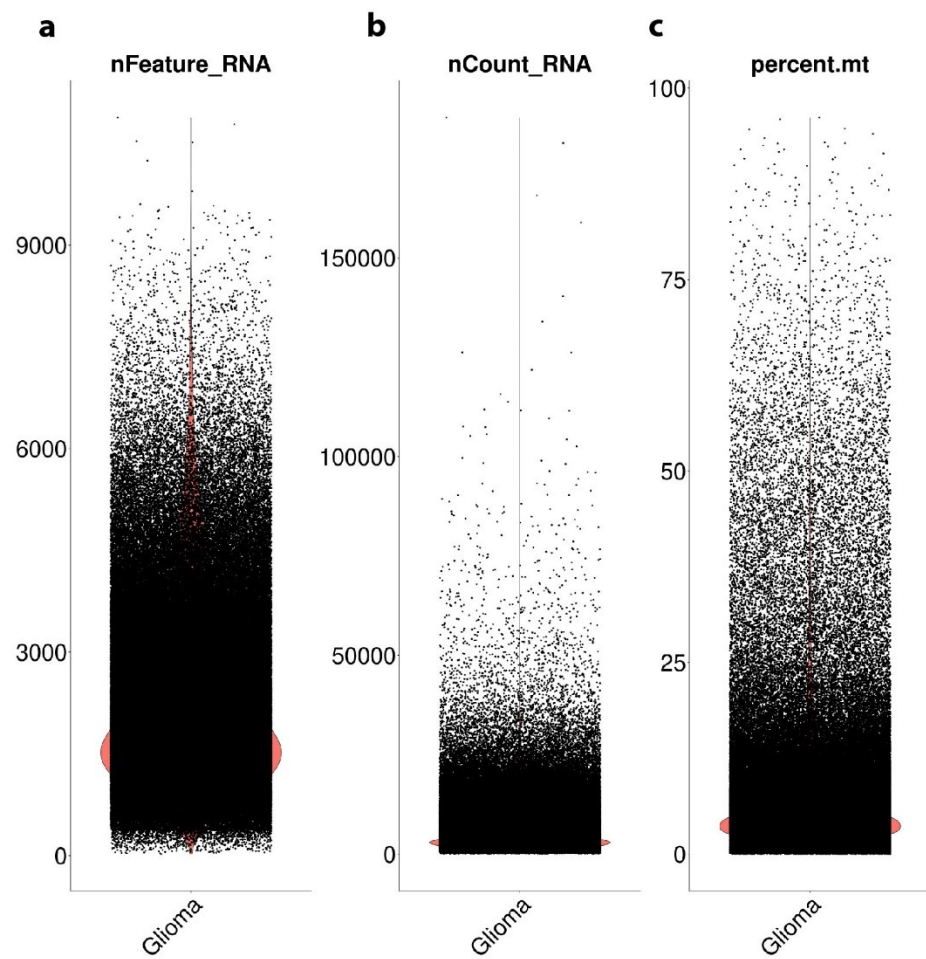
not consistent with the direct sequencing results of IDH, such as TP1 (G2), TP2 (G3), and TP17 (G1). The IDH status was preferentially determined by direct sequencing.

### Supplementary Fig.3



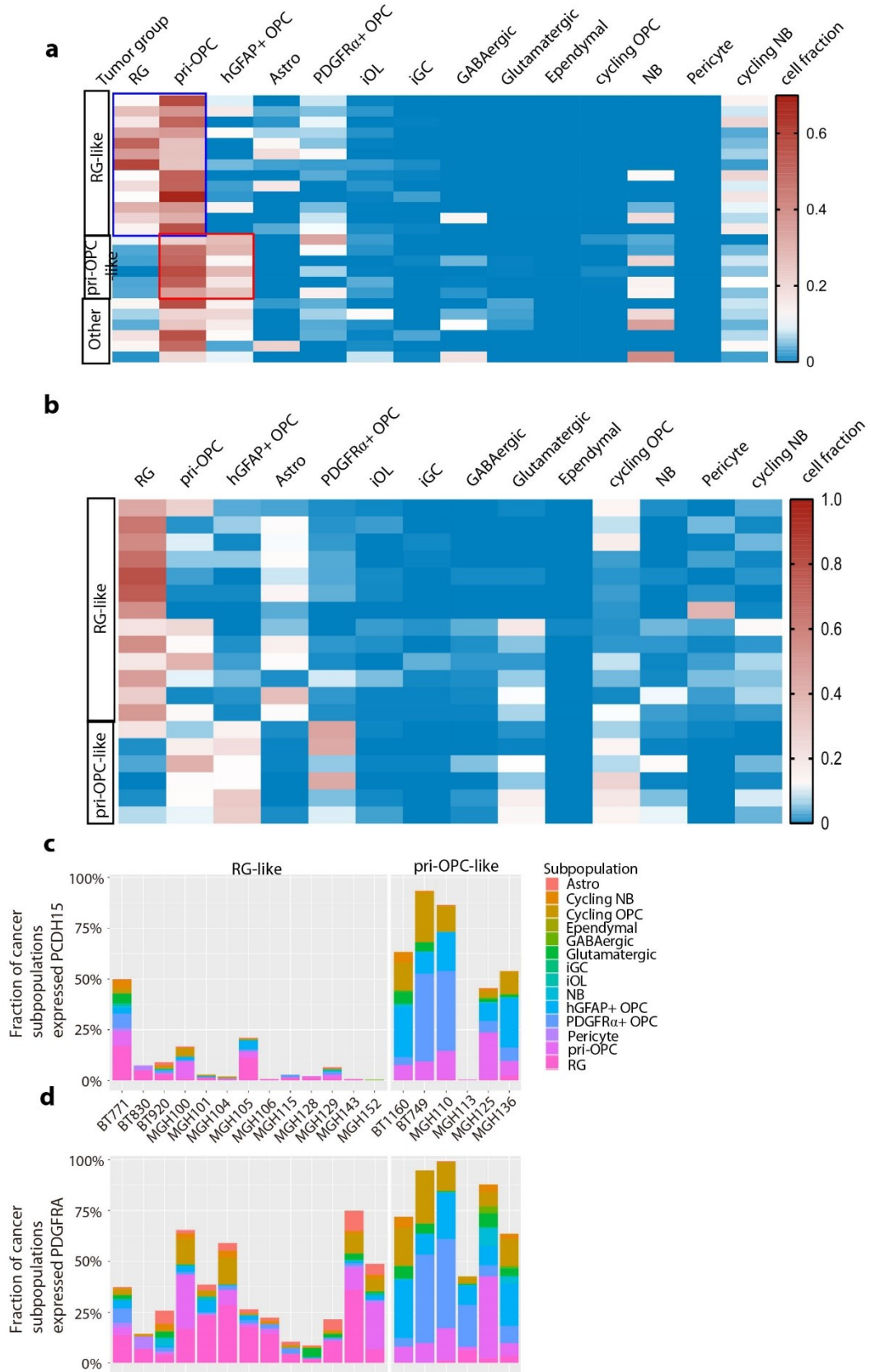
Supplementary Figure 3. **Single cell data from “fresh” and “thaw” methods are comparable.** A combination of methods as “fresh”, “thawed cells”, and “thawed tissue” was used mainly due to a waiting period of pathology results used for grouping. A comparison of “thaw” and “fresh” methods was performed (YL15 fresh vs YL21 thaw, YL17 fresh vs YL35 thaw). **a** Pearson’s correlation analysis between 50 randomly selected cells from “fresh” and “thaw” methods indicated a nice correlation between the two methods, with a correlation of near 1 in most cells. **b** Linear regression model was applied to compare average gene expression levels of data from “fresh” and “thaw” methods. The two methods had a nice correlation of mean expression,  $R^2=0.982$  or 0.974.

### Supplementary Fig.4



Supplementary Figure 4. **Plots of quality control metrics of all cells included in this study. a** Number of gene per cell detected. **b** Number of transcript (UMI) detected per cell. **c** Percentage of reads mapped to mitochondrial genes.

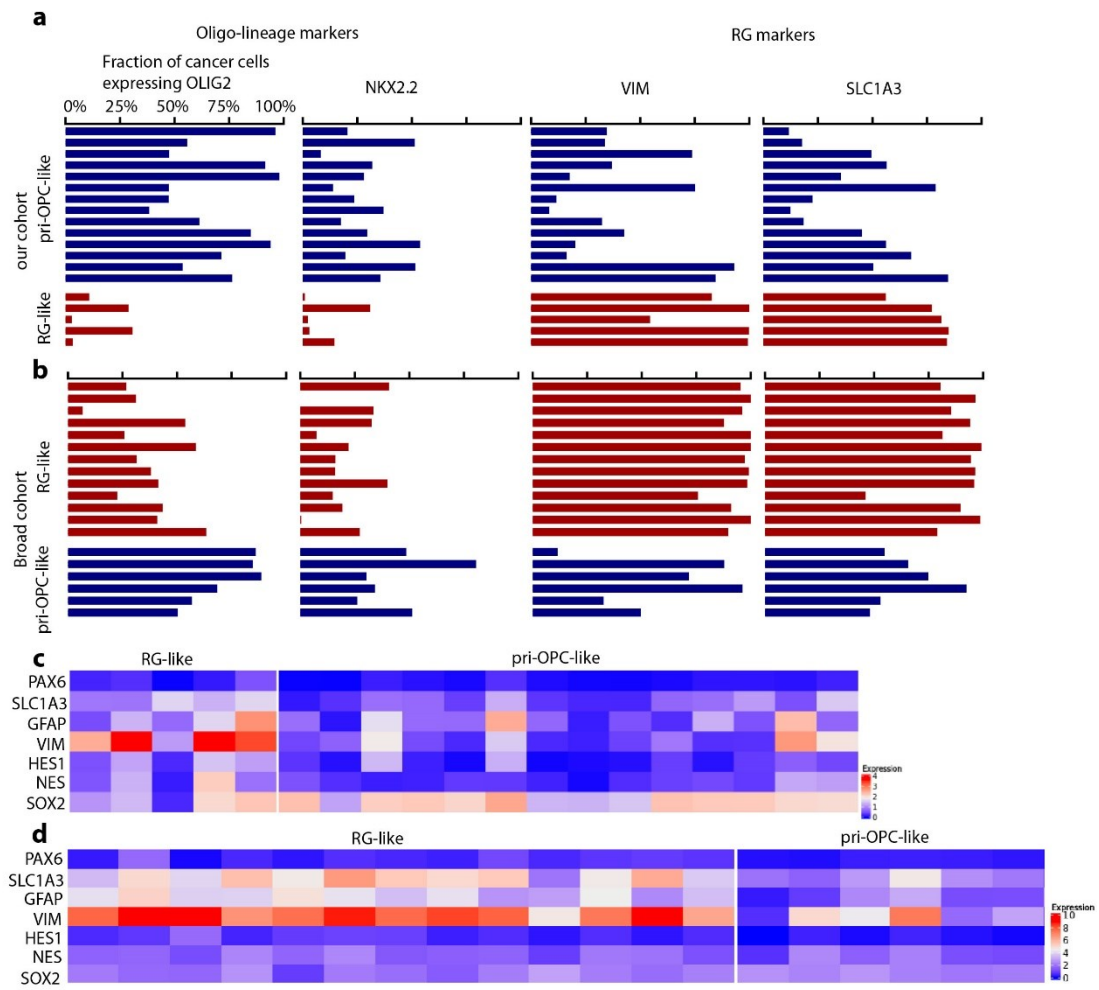
**Supplementary Fig.5**



Supplementary Figure 5. **Classification of RG-like and pri-OPC-like tumors validated in the Broad cohort.** **a** Heatmap of the Broad cohort matching to relative

abundance of mouse developmental cell types (hGFAP<sup>+</sup> and PDGFR $\alpha$ <sup>+</sup> lineages), computed by CIBERSORTx. Each row represented one patient. Totally 25 primary GBM samples were included. 13 and 6 of them were RG-like and pri-OPC-like tumors, respectively. The other 6 tumors were not assigned as RG-like nor pri-OPC-like and thus named as other tumors. **b** Similar mapping as **a** but computed by scmap. n=13 patients for RG-like tumors, n=6 patients for pri-OPC-like tumors. **c-d** a higher fraction of cancer subpopulations that expressed PCDH15 (c) and PDGFRA (d) was observed in pri-OPC-like tumors than that in RG-like ones.

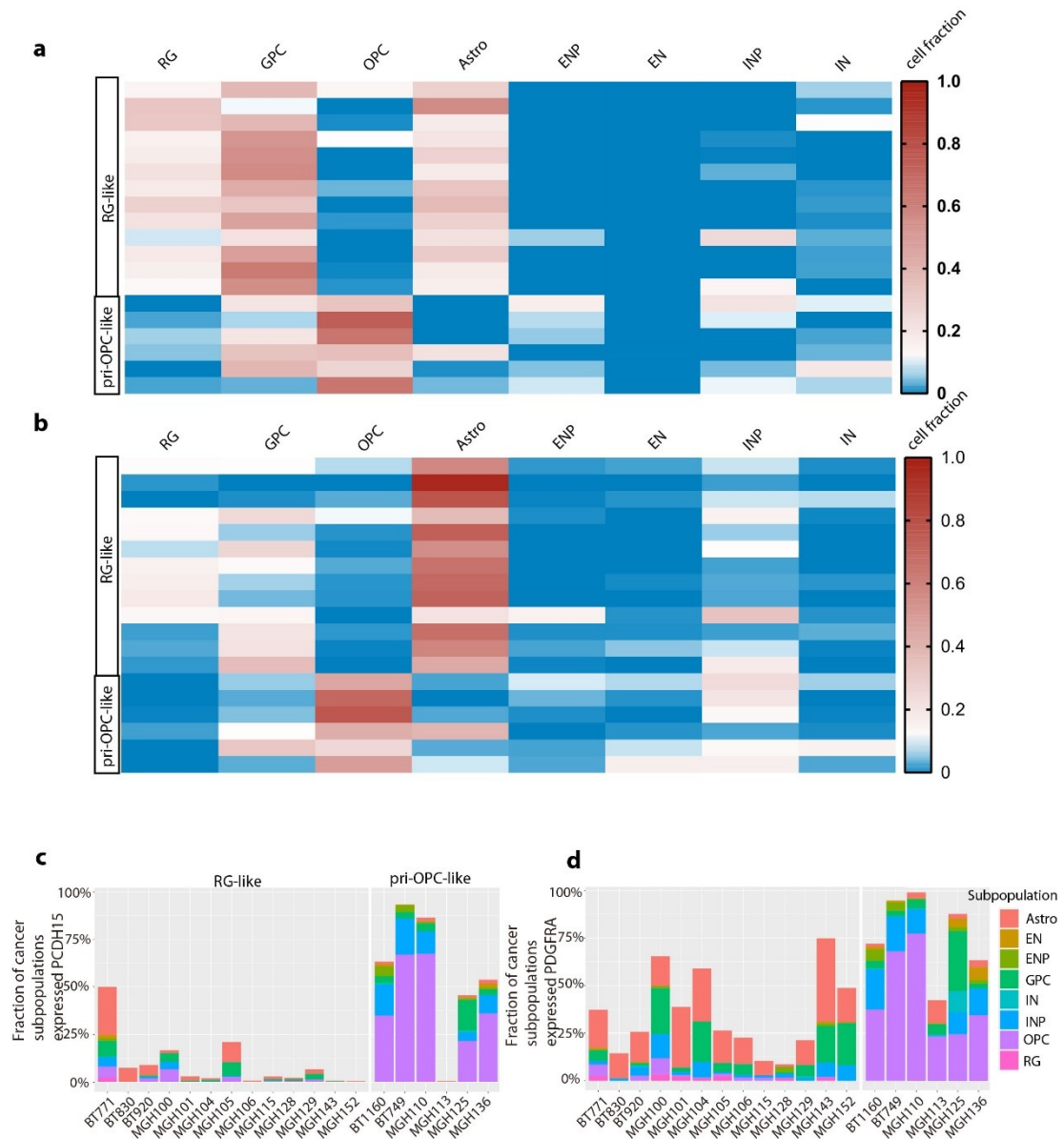
**Supplementary Fig.6**



Supplementary Figure 6. **Fraction of cancer cells that expressed other oligo-lineage and RG markers in each tumor from our and Broad cohorts.** **a** Fraction of all cancer cells that expressed oligo-lineage markers OLIG2/NKX2.2 and RG markers VIM/SLC1A3 in each patient from our cohort (n=5 patients for RG-like tumors, n=14 for pri-OPC-like tumors). **b** same as **a** but from Broad cohort (n=13 patients for RG-like tumors, n=6 for pri-OPC-like tumors). **c** Heatmap showing comparison of mean expression of RG marker genes (PAX6/SLC1A3/GFAP/VIM/HES1/NES/SOX2) between RG-like and pri-OPC-like tumors from our cohort. **d** same as **c** but from Broad cohort.



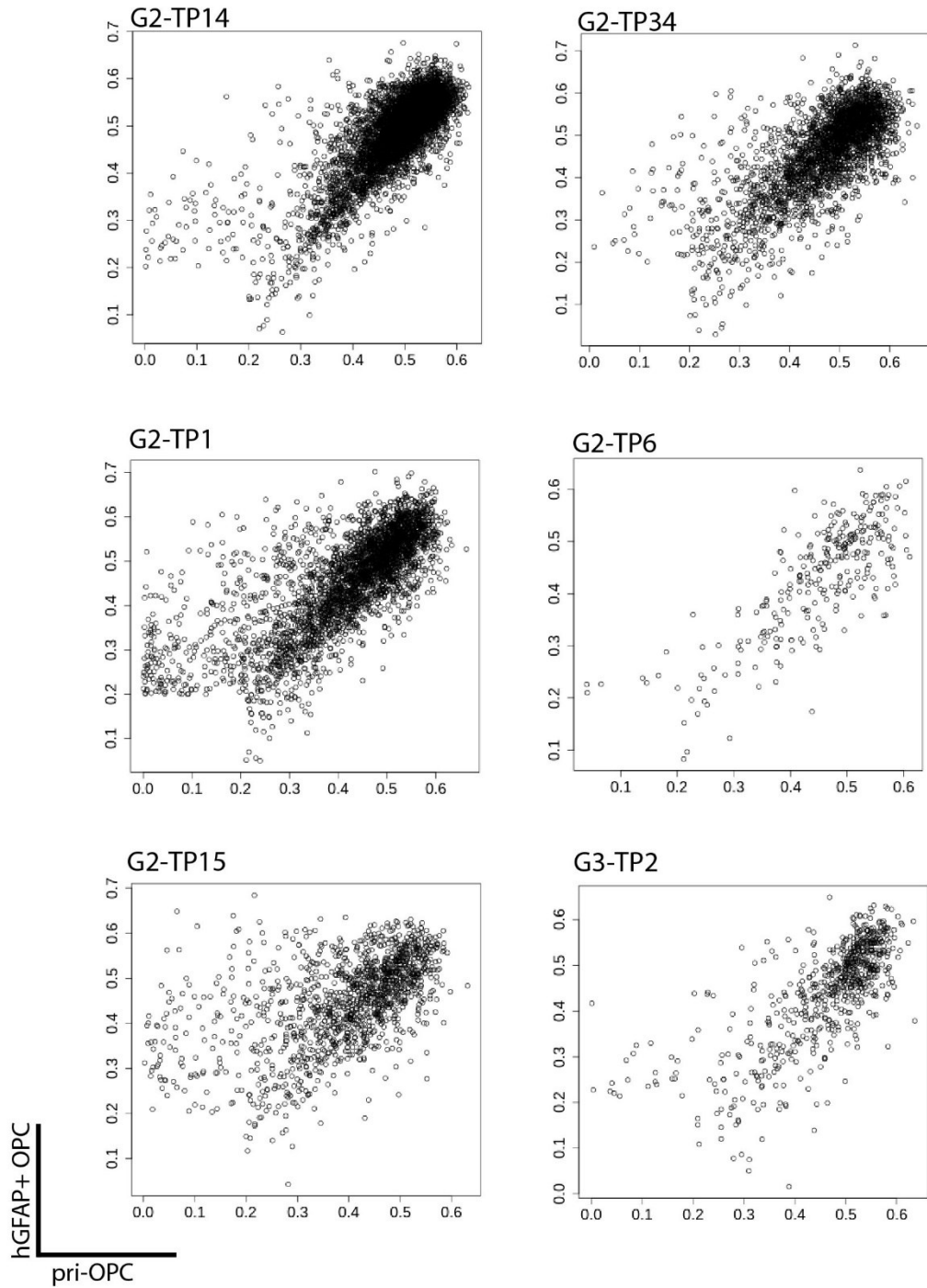
**Supplementary Fig.7**



Supplementary Figure 7. **Classification of RG-like and pri-OPC-like tumors was also robust in the Broad cohort.** **a** Heatmap of RG-like and pri-OPC-like tumors from the Broad cohort matching to relative abundance of human developmental cell types, computed by CIBERSORTx. n=13 patients for RG-like tumors, n=6 patients for pri-OPC-like tumors. Each row represented one patient. Note that RG-like tumors were most similar to GPCs, RGs and astrocytes, while pri-OPC-like tumors were most similar to OPCs. **b** Similar mapping as **a** but computed by scmap. Consistently with Fig.2b, the cancer subpopulations of RG-like and pri-OPC-like tumors were mapped to astrocytes/RGs and OPCs, respectively. **c-d** a higher fraction of cancer subpopulations

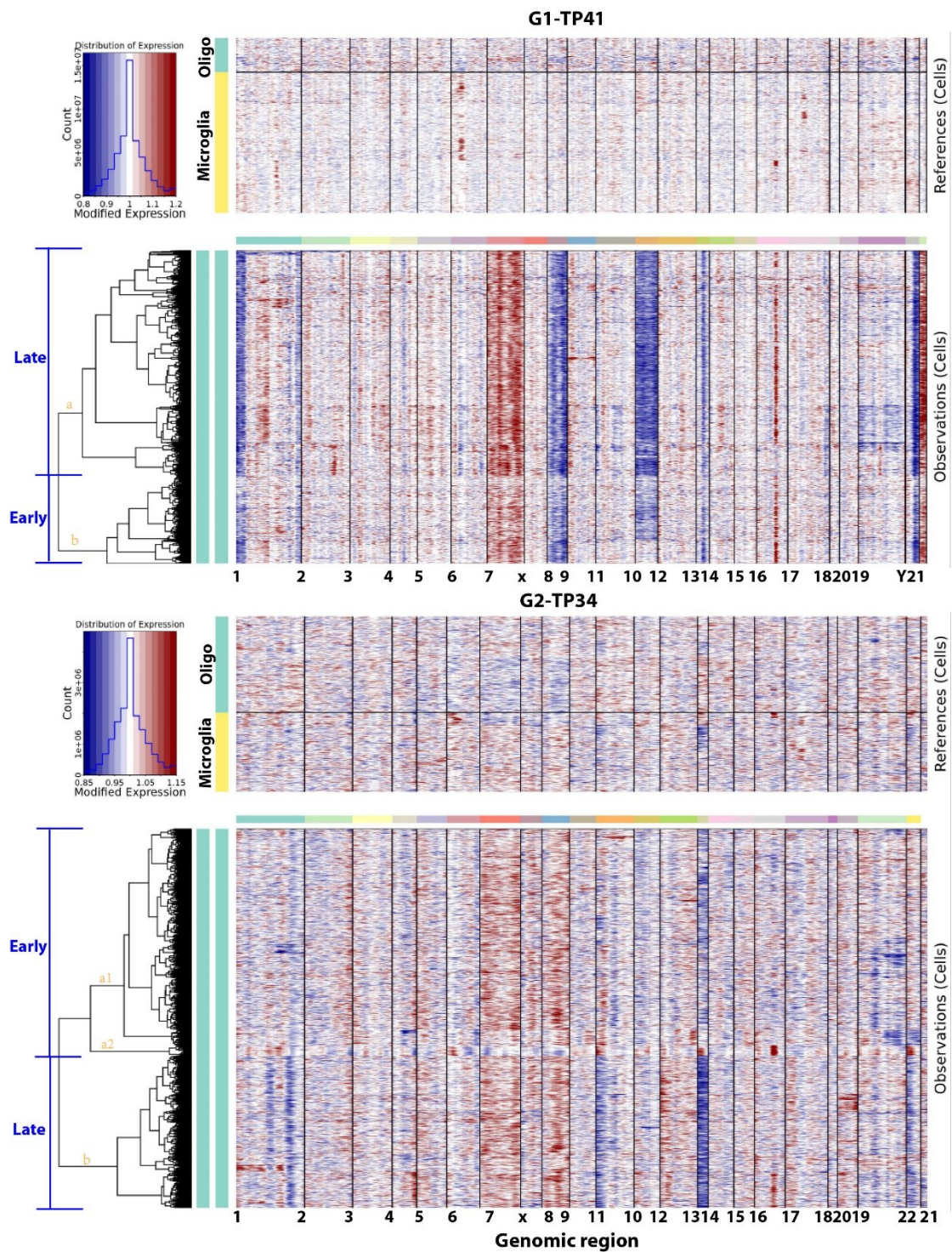
especially OPC-like subpopulations that expressed PCDH15 (c) and PDGFRA (d) was observed in pri-OPC-like tumors than that in RG-like ones.

## Supplementary Fig.8



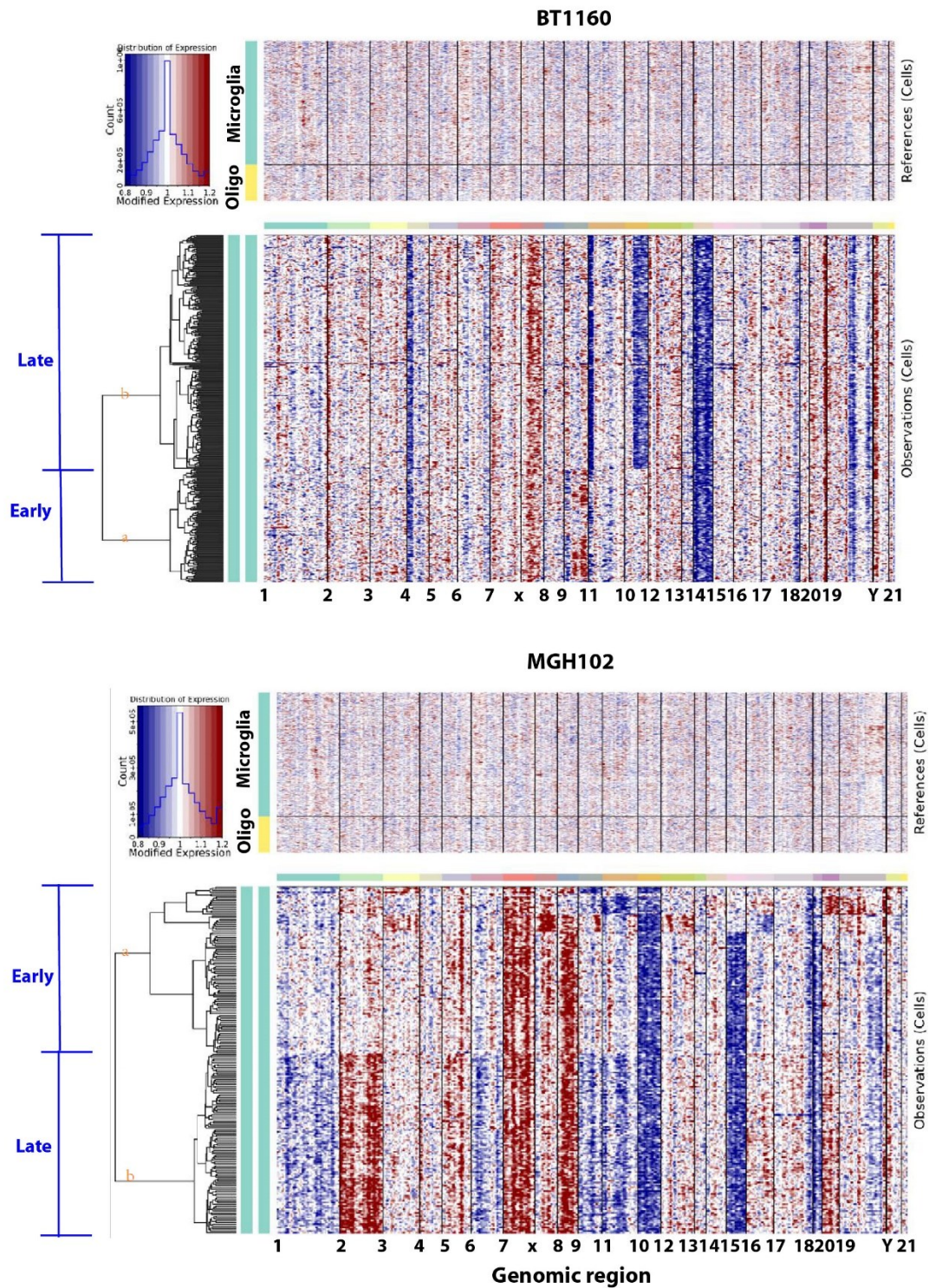
Supplementary Figure 8. **Pearson correlation analyses of two signatures on the same cancer cells.** Pearson correlation analysis was performed to show the correlation of signatures of two dominant cell types in the same cancer cells. Glioma samples (TP14, TP34, TP1, TP6, TP15, TP2) were shown.

Supplementary Fig.9



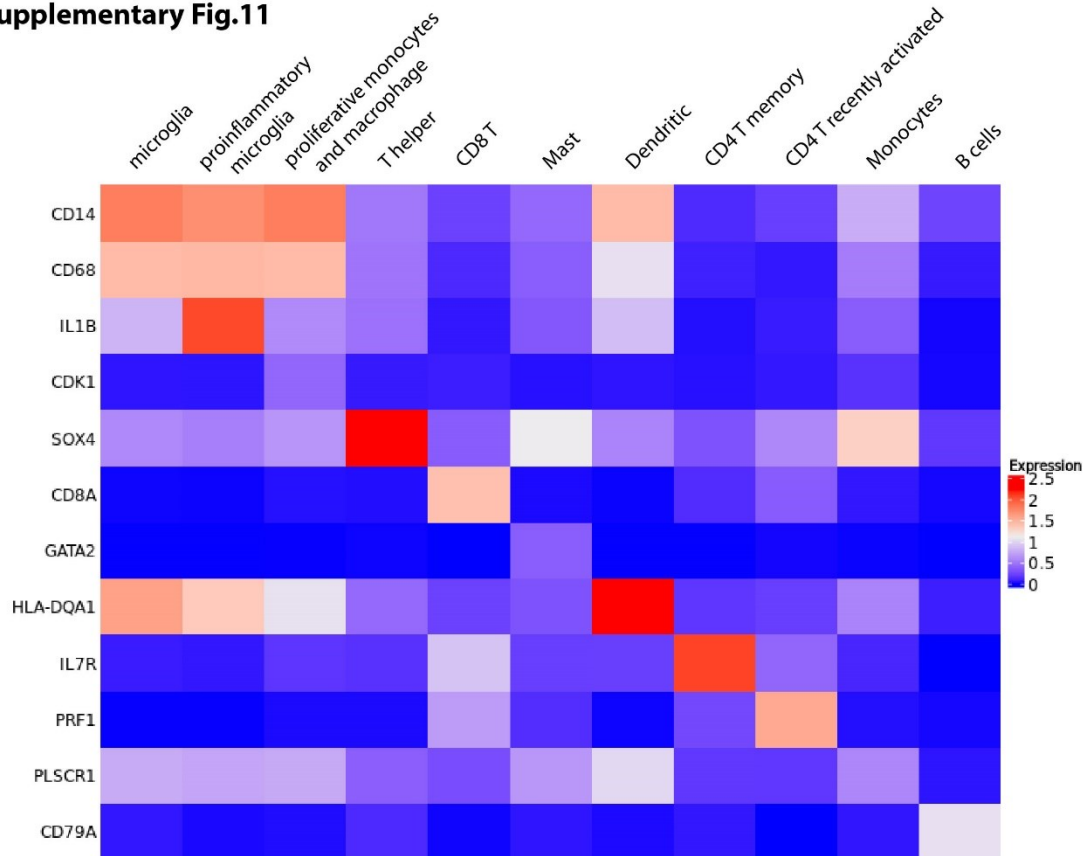
Supplementary Figure 9. **Inferred CNV profiles of scRNA seq dataset from our cohort.** Representative CNV profiles inferred from scRNA-Seq of patient #TP41 in G1 group and #TP34 in G2 group, respectively. Cells are ordered from non-cancer cells (oligodendrocytes, cyan-blue; microglia, yellow) to malignant cells (cyan-blue). Early and late subclones were indicated.

Supplementary Fig.10



Supplementary Figure 10. **Inferred CNV profiles of scRNA seq dataset from the public cohort.** Representative CNV profiles inferred from scRNA-Seq of patient #BT1160 and #MGH102, respectively. Cells are ordered from non-cancer cells (microglia, cyan-blue; oligodendrocyte, yellow) to malignant cells (cyan-blue). Early and late subclones were indicated.

## Supplementary Fig.11



Supplementary Figure 11. Heatmap of the markers used for tumor-infiltrating immune cell populations. Heatmap showing the expression of selected marker genes for each tumor infiltrating immune cell type. Selected markers of B cells ( $CD79A^1$ ), monocytes ( $PLSCR1^1$ ), dendritic cells ( $HLA-DQA1^1$ ), CD4 memory T cells ( $IL7R^2$ ), T helper cells ( $SOX4^3$ ), recently activated CD4 T cells (cytolytic gene  $PRF1^4$ ), and mast cells ( $GATA2^5$ ) were shown. CD14 and CD68 were used to label microglia. Proinflammatory microglia showed highest expression of proinflammatory gene  $IL1B^6$ . Proliferative monocytes and macrophage showed an expression of cell proliferative gene  $CDK1^7$ .

### Supplementary references

1. Franzén O, Gan L-M, Björkegren JLM. PanglaoDB: a web server for exploration of mouse and human single-cell RNA sequencing data. *Database*. 2019;2019. doi:10.1093/database/baz046
2. Kondrack RM, Harbertson J, Tan JT, McBreen ME, Surh CD, Bradley LM. Interleukin 7 regulates the survival and generation of memory CD4 cells. *J Exp Med*. 2003;198(12):1797-1806. doi:10.1084/jem.20030735

3. Kuwahara M, Yamashita M, Shinoda K, et al. The transcription factor Sox4 is a downstream target of signaling by the cytokine TGF- $\beta$  and suppresses T(H)2 differentiation. *Nat Immunol.* 2012;13(8):778-786. doi:10.1038/ni.2362
4. Cachot A, Bilous M, Liu Y-C, et al. Tumor-specific cytolytic CD4 T cells mediate immunity against human cancer. *Sci Adv.* 2021;7(9):eabe3348. doi:10.1126/sciadv.abe3348
5. Li Y, Gao J, Kamran M, et al. GATA2 regulates mast cell identity and responsiveness to antigenic stimulation by promoting chromatin remodeling at super-enhancers. *Nat Commun.* 2021;12(1):494. doi:10.1038/s41467-020-20766-0
6. Yeo AT, Rawal S, Delcuze B, et al. Single-cell RNA sequencing reveals evolution of immune landscape during glioblastoma progression. *Nat Immunol.* 2022;23(6):971-984. doi:10.1038/s41590-022-01215-0
7. Pepe G, De Maglie M, Minoli L, Villa A, Maggi A, Vegeto E. Selective proliferative response of microglia to alternative polarization signals. *J Neuroinflammation.* 2017;14(1):236. doi:10.1186/s12974-017-1011-6

Supplementary Table 1. Clinical information of 26 patients

Group#	TP#	Method	Gender	Age	Pathology	WHO grade	IDH1/2	1p19q	ATRX	TERT	TP53	MGMT promoter	BRAF	EGFR	PIK3CA
1	17	Thawed cells	F	28	Astrocytoma	4	WT	retain	WT	WT	WT	non-methylation	WT	WT	WT
1	36	Thawed tissue	F	42	Glioblastoma	4	WT	retain	WT	Mut	WT	non-methylation	WT	WT	WT
1	37	Thawed tissue	F	35	Glioblastoma	4	WT	retain	/	Mut	/	non-methylation	WT	/	/
1	43	Thawed tissue	M	16	Astrocytoma	4	WT	retain	Mut	WT	Mut	non-methylation	WT	WT	WT
1	03	Fresh	F	38	Glioblastoma	4	WT	co-del	WT	WT	Mut	non-methylation	WT	WT	WT
1	16	Fresh	M	61	Glioblastoma	4	WT	retain	/	Mut	/	non-methylation	Mut	WT	/
1	18	Thawed cells	M	56	Glioblastoma	4	WT	retain	WT	WT	WT	non-methylation	WT	WT	WT
1	32	Thawed tissue	M	57	Glioblastoma	4	WT	retain	/	Mut	/	non-methylation	WT	/	/
1	33	Thawed cells	M	68	Glioblastoma	4	WT	co-del	WT	Mut	WT	non-methylation	WT	WT	WT
1	41	Thawed tissue	M	57	Glioblastoma	4	WT	co-del	WT	Mut	Mut	non-methylation	WT	WT	WT
1	70	Thawed tissue	M	49	Glioblastoma	4	WT	retain	WT	Mut	WT	methylation	WT	Mut	Mut
2	14	Thawed cells	F	26	Astrocytoma	2	Mut	retain	WT	WT	Mut	methylation	WT	WT	WT
2	34	Thawed tissue	F	20	Astrocytoma	2	Mut	retain	WT	WT	Mut	non-methylation	WT	WT	WT
2	22	Thawed tissue	F	30	Astrocytoma	2	Mut	retain	/	WT	/	methylation	WT	/	/
2	19	Thawed tissue	M	38	Anaplastic Astrocytoma	3	Mut	retain	WT	WT	Mut	methylation	WT	WT	WT
2	30	Thawed tissue	M	29	Anaplastic Astrocytoma	3	Mut	retain	WT	WT	Mut	methylation	WT	WT	WT
2	1	Fresh	F	31	Astrocytoma	2	Mut	retain	Mut	WT	Mut	methylation	WT	WT	WT
2	4	Fresh	M	42	Astrocytoma	2	Mut	retain	/	WT	/	non-methylation	WT	/	/
2	6	Fresh	M	29	Astrocytoma	2	Mut	retain	/	WT	/	methylation	WT	/	/



2	11	Fresh	M	39	Astrocytoma	2	Mut	retain	/	WT	/	non-methylation	WT	/	/
2	15	Fresh	F	56	Astrocytoma	2	Mut	retain	WT	WT	Mut	methylation	WT	WT	WT
3	2	Fresh	M	46	Oligodendroglioma	2	Mut	co-del	/	Mut	/	methylation	WT	/	/
3	8	Fresh	F	48	Oligodendroglioma	2	Mut	co-del	WT	Mut	WT	methylation	WT	WT	WT
3	28	Thawed tissue	F	37	Oligodendroglioma	2	Mut	co-del	/	Mut	/	methylation	WT	/	/
3	59	Thawed tissue	F	39	Oligodendroglioma	2	Mut	co-del	/	Mut	/	methylation	WT	/	/
3	62	Thawed tissue	M	42	Oligodendroglioma	3	Mut	co-del	WT	WT	Mut	methylation	WT	WT	WT

Supplementary Table 2. QC data of the 26 samples by 10x single cell RNA seq

Group#	TP #	Estimated cell number	Mean Reads per Cell	Median Genes per Cell	Number of Reads	Valid Barcodes	Sequencing Saturation	Q30 Bases in Barcode	Q30 Bases in RNA Read	Q30 Bases in Sample Index	Reads Mapped to Genome	Reads Mapped Confidently to Genome	Reads Mapped Confidently to Intergenic Regions	Reads Mapped Confidently to Intronic Regions	Reads Mapped Confidently to Exonic Regions	Reads Mapped Confidently to Transcriptome	Reads Mapped Antisense to Gene	Fraction Reads in Cells	Total Genes Detected	Median UMI Count per Cell
1	17	7,859	51,065	2,667	401,327,587	97.20%	45.50%	94.60%	90.50%	93.30%	93.40%	89.90%	5.00%	21.90%	62.90%	59.30%	1.60%	73.20%	24,375	10,089
1	36	6,712	91,925	1,347	617,002,960	95.40%	84.40%	95.90%	91.90%	95.70%	93.90%	90.70%	8.10%	35.50%	47.10%	43.50%	1.70%	66.50%	23,479	2,579
1	37	8,484	89,965	1,548	763,267,744	96.20%	86.70%	95.80%	90.90%	89.50%	93.90%	90.90%	5.60%	27.70%	57.60%	54.20%	1.30%	80.30%	24,105	3,758
1	43	8,725	59,415	1,719	518,396,245	96.20%	78.00%	95.80%	90.10%	95.50%	93.70%	90.80%	7.10%	33.70%	49.90%	46.30%	1.40%	83.70%	24,491	3,646
1	3	3,253	136,859	3,275	445,204,725	97.80%	74.20%	95.90%	91.90%	92.70%	94.40%	91.60%	5.80%	21.30%	64.50%	60.70%	1.50%	68.30%	23,824	10,358
1	16	2,172	204,686	4,227	444,578,400	98.00%	71.40%	96.00%	92.50%	93.10%	94.60%	92.00%	3.70%	18.90%	69.30%	65.80%	1.30%	71.80%	23,810	19,314
1	18	14,040	48,964	3,206	687,463,160	97.00%	46.70%	97.10%	95.30%	95.90%	96.00%	91.90%	6.60%	30.80%	54.50%	49.90%	2.30%	87.40%	25,797	9,671
1	32	7,446	48,753	1,300	363,016,160	97.20%	74.20%	96.70%	94.00%	94.60%	94.50%	88.30%	9.50%	34.10%	44.70%	40.70%	2.10%	88.90%	24,331	3,080
1	33	20,969	44,909	3,219	941,717,465	96.70%	43.30%	97.10%	95.00%	96.00%	95.60%	90.90%	5.60%	25.00%	60.20%	54.90%	2.70%	83.90%	26,923	9,673
1	41	16,096	46,369	2,753	746,369,041	96.40%	51.00%	96.90%	94.20%	95.40%	95.10%	90.20%	5.70%	27.40%	57.10%	51.70%	2.70%	87.30%	27,499	7,842
1	70	19,069	50,128	2,512	955,907,403	96.70%	57.80%	97.10%	95.30%	96.90%	95.90%	90.90%	8.80%	36.90%	45.20%	40.40%	2.80%	84.10%	27,961	5,552
2	14	8,848	48,860	2,445	432,320,607	97.40%	59.00%	94.70%	90.70%	91.30%	93.70%	90.30%	5.10%	26.20%	59.00%	55.50%	1.50%	77.50%	23,845	6,956
2	34	5,159	97,895	2,004	505,044,491	95.20%	73.30%	95.70%	91.30%	95.50%	94.00%	90.70%	6.70%	35.50%	48.50%	44.80%	1.70%	59.00%	24,092	4,455
2	22	11,597	53,065	1,493	615,405,631	96.50%	78.90%	95.70%	90.40%	95.50%	93.40%	90.50%	5.30%	34.60%	50.60%	47.10%	1.30%	82.80%	23,992	3,256
2	19	11,360	46,852	1,864	532,244,902	96.50%	71.90%	95.90%	90.40%	95.60%	94.00%	91.10%	5.30%	31.30%	54.50%	50.80%	1.30%	87.10%	23,894	4,620
2	30	9,829	58,436	1,990	574,372,121	96.80%	70.20%	96.00%	91.10%	95.70%	95.00%	92.10%	4.50%	19.40%	68.20%	64.50%	1.10%	82.60%	23,069	7,202

2	1	11,201	40,161	1,846	449,854,194	97.40%	64.20%	96.20%	92.50%	85.50%	93.30%	90.00%	4.90%	22.40%	62.60%	58.70%	1.80%	67.10%	24,515	4,322
2	4	9,772	50,875	2,276	497,155,879	97.40%	62.70%	96.20%	92.80%	93.70%	94.70%	91.70%	6.20%	27.60%	57.90%	54.10%	1.80%	77.80%	24,734	6,280
2	6	953	385,160	2,353	367,057,559	98.00%	94.40%	96.10%	91.50%	94.70%	93.10%	89.80%	5.90%	29.00%	54.80%	51.40%	1.50%	79.00%	21,455	5,606
2	11	332	672,919	1,947	223,409,120	97.90%	96.40%	95.60%	91.20%	94.50%	92.70%	88.30%	5.60%	29.80%	53.00%	50.00%	1.40%	65.30%	18,698	4,535
2	15	4,450	87,125	2,253	387,709,750	97.90%	75.20%	96.00%	92.40%	93.00%	94.30%	91.30%	5.60%	29.30%	56.50%	52.90%	1.70%	77.00%	23,324	6,351
3	2	2,827	133,374	2,562	377,049,997	97.30%	79.30%	96.20%	92.50%	95.30%	94.40%	91.60%	4.00%	19.60%	67.90%	64.10%	1.60%	54.40%	22,932	6,471
3	8	3,053	138,029	1,970	421,404,910	97.90%	87.50%	96.20%	91.40%	93.10%	93.00%	89.90%	5.50%	27.10%	57.40%	53.80%	1.60%	65.80%	22,971	4,170
3	28	15,607	49,703	2,536	775,718,178	96.60%	50.20%	97.10%	95.20%	92.10%	96.40%	92.70%	9.20%	44.50%	39.00%	34.80%	2.40%	84.50%	26,913	5,548
3	59	12,569	52,730	1,555	662,763,815	96.60%	64.00%	97.00%	94.70%	96.40%	95.60%	89.70%	10.60%	34.40%	44.70%	40.10%	2.70%	70.70%	26,091	3,843
3	62	2,285	130,621	1,657	298,470,826	96.10%	83.60%	96.70%	94.00%	95.10%	96.40%	92.70%	8.30%	36.30%	48.10%	43.60%	2.50%	69.10%	22,876	3,359

Supplementary Table 3. Network analysis of TCGA samples

Modules related to EGFR (RG-like tumors)				
Driver Gene	Module ID	Gene Count	Term	Adjusted P Value
EGFR	c1_28	19	positive regulation of epidermal growth factor-activated receptor activity (GO:0045741)	0.033011845
EGFR	c1_259	17	epidermal growth factor receptor binding (GO:0005154)	0.040426373
EGFR	c1_286	10	positive regulation of epidermal growth factor receptor signaling pathway (GO:0045742)	0.024107021

EGFR	c1_306	23	cellular response to epidermal growth factor stimulus (GO:0071364)	0.038810058
EGFR	c1_311	13	cellular response to epidermal growth factor stimulus (GO:0071364)	0.034300946
EGFR	c1_311	13	epidermal growth factor receptor signaling pathway (GO:0007173)	0.047735528
EGFR	c1_441	14	epidermal growth factor receptor binding (GO:0005154)	0.036128792
EGFR	c1_441	14	positive regulation of epidermal growth factor-activated receptor activity (GO:0045741)	0.038486831
EGFR	c1_498	17	regulation of epidermal growth factor receptor signaling pathway (GO:0042058)	0.036891098
EGFR	c1_632	12	epidermal growth factor receptor signaling pathway (GO:0007173)	0.044120661
EGFR	c1_638	33	regulation of epidermal growth factor receptor signaling pathway (GO:0042058)	0.044629028
EGFR	c1_668	78	cellular response to epidermal growth factor stimulus (GO:0071364)	0.04184305
EGFR	c1_788	21	epidermal growth factor receptor binding (GO:0005154)	0.042904043
EGFR	c1_795	29	positive regulation of epidermal growth factor-activated receptor activity (GO:0045741)	0.042891451
EGFR	c1_896	23	regulation of epidermal growth factor receptor signaling pathway (GO:0042058)	0.03630385
EGFR	c1_1009	17	cellular response to epidermal growth factor stimulus (GO:0071364)	0.037737473

EGFR	c1_1017	11	epidermal growth factor receptor binding (GO:0005154)	0.02788898
EGFR	c1_1099	12	epidermal growth factor receptor signaling pathway (GO:0007173)	0.043711864
Modules related to LRP1B (RG-like tumors)				
Driver Gene	Module ID	Gene Count	Term	Adjusted P Value
LRP1B	c1_3	4931	receptor complex (GO:0043235)	6.31433E-08
LRP1B	c1_14	2989	receptor complex (GO:0043235)	0.029005523
Modules related to TP53 (pri-OPC-like tumors)				
Driver Gene	Module ID	Gene Count	Term	Adjusted P Value
TP53	c1_6	798	regulation of signal transduction by p53 class mediator (GO:1901796)	1.48417E-06
TP53	c1_6	798	DNA damage response, signal transduction by p53 class mediator resulting in cell cycle arrest (GO:0006977)	6.73318E-06
TP53	c1_6	798	DNA damage response, signal transduction by p53 class mediator resulting in transcription of p21 class mediator (GO:0006978)	0.014896876
TP53	c1_23	300	intrinsic apoptotic signaling pathway by p53 class mediator (GO:0072332)	0.021780802
TP53	c1_46	10	DNA damage response, signal transduction by p53 class mediator (GO:0030330)	0.026522

TP53	c1_74	378	regulation of signal transduction by p53 class mediator (GO:1901796)	9.47E-08
TP53	c1_74	378	DNA damage response, signal transduction by p53 class mediator resulting in cell cycle arrest (GO:0006977)	5.72E-06
TP53	c1_74	378	DNA damage response, signal transduction by p53 class mediator resulting in transcription of p21 class mediator (GO:0006978)	0.000794772
TP53	c1_82	33	positive regulation of DNA damage response, signal transduction by p53 class mediator (GO:0043517)	0.004919108
TP53	c1_83	23	intrinsic apoptotic signaling pathway by p53 class mediator (GO:0072332)	0.040857606
TP53	c1_222	18	positive regulation of DNA damage response, signal transduction by p53 class mediator (GO:0043517)	0.030383253
TP53	c1_222	18	intrinsic apoptotic signaling pathway by p53 class mediator (GO:0072332)	0.046847432
TP53	c1_242	32	negative regulation of intrinsic apoptotic signaling pathway in response to DNA damage by p53 class mediator (GO:1902166)	0.049033719
TP53	c1_242	32	negative regulation of DNA damage response, signal transduction by p53 class mediator (GO:0043518)	0.049632126
TP53	c1_276	10	negative regulation of intrinsic apoptotic signaling pathway in response to DNA damage by p53 class mediator (GO:1902166)	0.02115308
TP53	c1_276	10	negative regulation of DNA damage response, signal transduction by p53 class mediator (GO:0043518)	0.02115308
TP53	c1_282	28	DNA damage response, signal transduction by p53 class mediator resulting in transcription of p21 class mediator (GO:0006978)	0.038700106
TP53	c1_365	330	regulation of signal transduction by p53 class mediator (GO:1901796)	1.58E-08

TP53	c1_365	330	DNA damage response, signal transduction by p53 class mediator resulting in cell cycle arrest (GO:0006977)	1.64E-06
TP53	c1_365	330	DNA damage response, signal transduction by p53 class mediator resulting in transcription of p21 class mediator (GO:0006978)	0.000430114
TP53	c1_392	19	intrinsic apoptotic signaling pathway by p53 class mediator (GO:0072332)	0.039618997
TP53	c1_417	18	negative regulation of intrinsic apoptotic signaling pathway in response to DNA damage by p53 class mediator (GO:1902166)	0.029876999
TP53	c1_417	18	negative regulation of DNA damage response, signal transduction by p53 class mediator (GO:0043518)	0.029876999
TP53	c1_435	23	intrinsic apoptotic signaling pathway by p53 class mediator (GO:0072332)	0.038253339
TP53	c1_579	15	negative regulation of intrinsic apoptotic signaling pathway in response to DNA damage by p53 class mediator (GO:1902166)	0.023104954
TP53	c1_579	15	negative regulation of DNA damage response, signal transduction by p53 class mediator (GO:0043518)	0.023104954
TP53	c1_707	165	DNA damage response, signal transduction by p53 class mediator resulting in cell cycle arrest (GO:0006977)	1.84E-05
TP53	c1_707	165	regulation of signal transduction by p53 class mediator (GO:1901796)	0.006475418
TP53	c1_707	165	DNA damage response, signal transduction by p53 class mediator resulting in transcription of p21 class mediator (GO:0006978)	0.027380668
TP53	c1_708	114	regulation of signal transduction by p53 class mediator (GO:1901796)	0.000189883
TP53	c1_708	114	DNA damage response, signal transduction by p53 class mediator resulting in transcription of p21 class mediator (GO:0006978)	0.01683666

TP53	c1_709	15	DNA damage response, signal transduction by p53 class mediator resulting in cell cycle arrest (GO:0006977)	0.009092862
TP53	c1_808	16	intrinsic apoptotic signaling pathway by p53 class mediator (GO:0072332)	0.026859966
TP53	c1_886	84	regulation of signal transduction by p53 class mediator (GO:1901796)	0.000346021
TP53	c1_960	52	intrinsic apoptotic signaling pathway in response to DNA damage by p53 class mediator (GO:0042771)	0.037912319